

## P9R.4 AN EXTENSIVE VALIDATION EXPERIMENT OF ALGORITHM ZPHI APPLIED TO RADAR HYDRIX

E. Le Bouar<sup>1</sup>, E. Moreau<sup>1</sup>, J. Testud<sup>1</sup>, H. Poulima<sup>1</sup>, R. Ney<sup>2</sup>, O. Deudon<sup>3</sup>

<sup>1</sup>NOVIMET, Vélizy, France

<sup>2</sup>Centre d'étude des Environnements Terrestre et Planétaires, Saint-Maur-des-Fossés, France

<sup>3</sup>ARVALIS Institut du Végétal, Boigneville, France

### 1. INTRODUCTION

Since September 2004, Hydrix radar has been in operation at the site of ARVALIS-Institut-du-Végétal in Beauce (France). Hydrix is a compact X-band polarimetric radar devoted to hydrological applications. Its primary data (reflectivity factor, differential phase shift, differential reflectivity and correlation coefficient) are processed in real time by the rain profiling algorithm ZPHI (Testud et al., 2000) to deliver both rainfall rate R and the DSD intercept parameter  $N0^*$ .

The main benefits of ZPHI lie in its capability to correct for attenuation and to deal with rain variability, even with short dwell times. The latter aspect is quite relevant, since it allows X-band radars to be used in operational conditions, especially with fast scanning.

While this algorithm has ever been validated with recorded data (e.g. Le Bouar et al., 2001 and Iwanami et al., 2003), direct results from real-time processing have been strongly missing.

The operating radar, neighbored by a rain gauge network, now provides the opportunity to test and validate the Hydrix system as the first one using ZPHI during operation.

### 2. EXPERIMENTAL SET-UP

The radar scanning zone is a single elevation azimuth sector spanning from 200° to 275°, with a maximum range of 60km. The 3 deg/s antenna speed ensures a revisit time less than 30 s long in average.

To capture rain during cold seasons, the exploration is performed at a low elevation angle. Initially, this elevation was set to 1.5°, but top of trees located a few tens of meter in front of the radar caused significant partial beam

filling from 200° to 235° azimuth. To reduce such an effect, the antenna elevation was raised to 2.2° at end of October 2004.

The radar coverage sector overflows 24 tipping bucket gauges, 8 of which are located within the partially masked zone. This gauge network is spread quite close to the radar, with a maximum distance of 25 km far from the radar.

An optical spectro-pluviometer (OSP) from CETP was installed too, to measure the local drop size distribution, and to provide a local statistics of  $N0^*$ , useful for radar calibration issues.

### 3. PARTIAL BEAM FILLING CORRECTION

Partial beam filling causes negative bias on reflectivity measurements, and then leads to  $N0^*$  overestimation in ZPHI. One can take advantage of this to deduce the corresponding reflectivity bias, by comparing  $N0^*$  statistics derived from ZPHI and the one derived from DSD measurements, as illustrated in Le Bouar et al. (2001).

In the case of partial mask feature, such statistics are to be performed directionally. Admitting that the statistics derived from the OSP is representative of the whole domain explored by the radar, a reference is then given for each azimuth.

Fig. 1(a) and (b) show the  $N0^*$  statistics obtained every 0.5° azimuth, at elevations 1.5° and 2.2° respectively. Considering the resulting reflectivity correction maps superimposed on these figures, one can notice the strong corrections within the 200°-235° azimuth sector, with a maximum of 9 dB at 225° azimuth at the lowest elevation angle. As expected, the correction values prescribed at 2.2° elevation are much weaker.

### 4. RADAR-GAUGE COMPARISONS

To make them comparable, both gauge and radar data were preliminarily transformed: Gauge measurements, originally obtained with a

---

\* Corresponding author address: Erwan Le Bouar, NOVIMET, 10-12, avenue de l'Europe, 78140 Vélizy, France; e-mail: [lebouar@novimet.com](mailto:lebouar@novimet.com).

6min-time resolution, were integrated to produce one-hour rainfall. Meanwhile, radar-derived rainfall rate were projected on a Cartesian grid with 1kmx1km resolution, and then were integrated over a 1hr time interval.

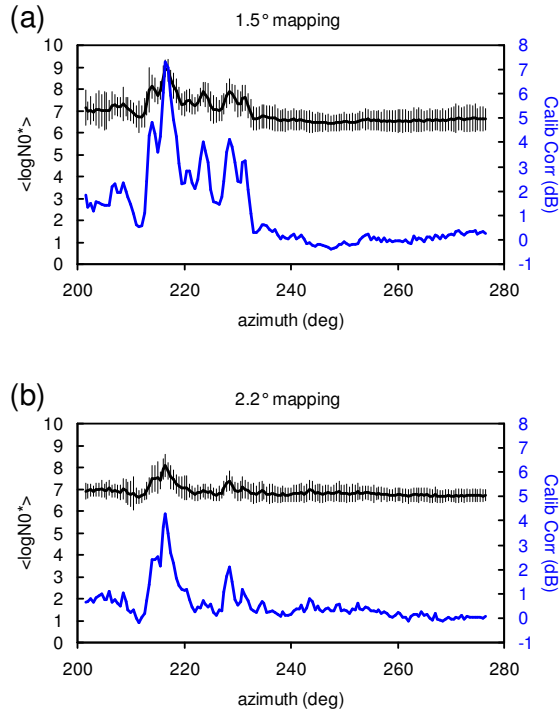


Figure 1: Azimuth-by-azimuth  $N0^*$  statistics (black, mean with standard deviation bars) and resulting calibration correction map (blue). (a) At  $1.5^\circ$  elevation; (b) at  $2.2^\circ$  elevation.

Each comparison involves monthly gathered data, providing six case studies. For illustration, two of them are plotted in Fig. 2 and 3. The black plots stand for ZPHI retrieval compared with rain gauge. For reference, comparison between gauge and rainfall classically retrieved are plotted in grey. The classical retrieval (referenced as Z-R hereafter) converts the reflectivity uncorrected for attenuation into rainfall rate. The Z-R law used ( $Z=268R^{1.69}$ ) has been chosen to be representative of the local climatology. Differences observed between ZPHI-gauge and (Z-R)-gauge plots may result from attenuation correction mainly.

Analysis of the six comparison cases is summarized in Fig. 4, 5 and 6. In each figure, four comparisons are considered: ZPHI- and (Z-R)-gauge comparison applied to the whole gauge network, and ZPHI- and (Z-R)-gauge

comparison excluding gauges located in the partially masked zone.

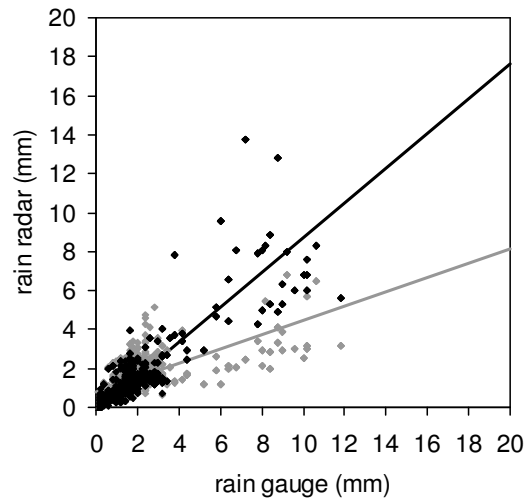


Figure 2: October 2004 radar vs. gauge comparison plots, with their orthogonal linear fits. ZPHI plot (black) and (Z-R) plot (grey).

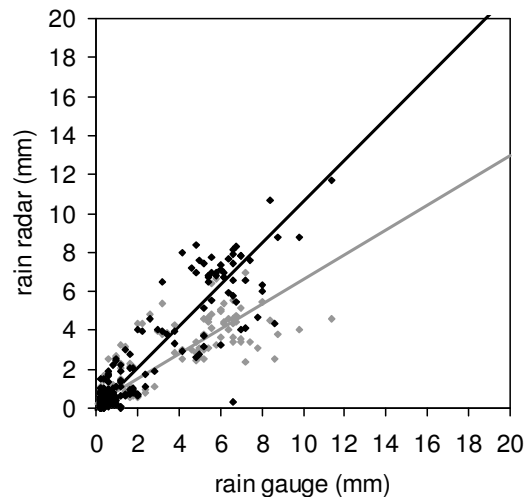


Figure 3: Same as Fig.2, but for July 2005.

Orthogonal linear fit slopes are shown in Fig. 4. Apart from the not-masked case of April 2005, most of ZPHI-gauge slopes approach unity. For March 2005, (Z-R)-gauge plot characteristics are virtually identical with those of ZPHI-gauge one, suggesting negligible attenuation during the rain events.

Radar-gauge agreement may be supported by Pearson correlation and Nash coefficients for all but one of the months considered (see fig. 5 and 6). Because the reflectivity correction is less

steady in partial mask zone, the *not-masked* data set coefficients are slightly better than the *overall* data set ones. The downward trend observed for both coefficients is thought to originate from the changing structures of rain cells getting less stratiform, and more sparsely convective from spring to summer. Although it is minimized by small distances between gauge and radar and small antenna elevation, representativeness error may be increased by spatial and time rain variability. Note that this includes gauge measurement errors as part of plot scattering sources.

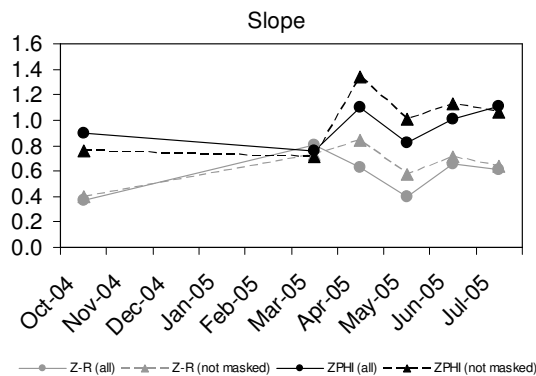


Figure 4: Slopes of orthogonal linear fits for six monthly comparison cases between gauge and radar rainfalls. Black symbols refer to ZPHI, and grey ones to (Z-R). Circles stand for the overall gauge network, and triangles for the gauges outside the partial mask zone.

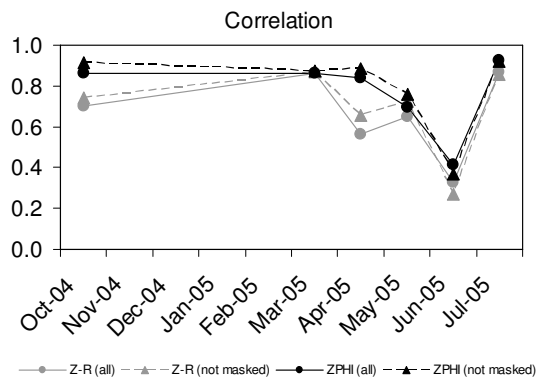


Figure 5: Pearson correlation coefficient for the six monthly comparison cases.

Pearson and Nash coefficients for June 2005 show a significantly bad agreement between radar and gauge measurements. Such discrepancy can be explained at least in part by strong precipitation events, inducing both

underestimation and overestimation of rainfall by ZPHI, thus leading to a much more scattered plot. Indeed, much of explanation for the underestimation of rainfall rests with mixed rain-hail occurrence and signal extinction. In contrast, overestimated rainfall value may result from negative reflectivity bias caused by antenna watering.

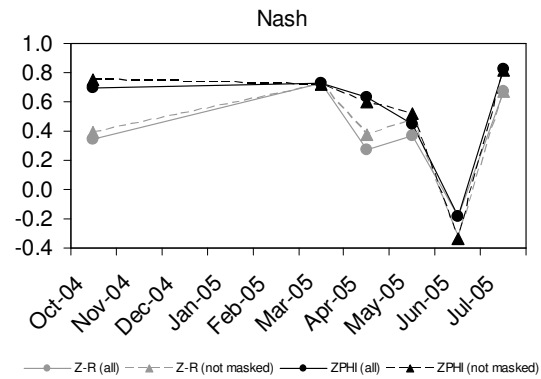


Figure 5: Nash coefficient for the six monthly comparison cases.

## 6. CONCLUSION

One of the objectives of the experiment set up at the site of Arvals-Institut-du-Végétal has been validating the rainfall measured by the "Hydrix+ZPHI" radar system, compared with that measured by a network of 24 rain gauges.

The preliminary results presented in this paper show some good agreement between the radar rainfall and the gauge measurements, apart from June 2005. However the validation study, still in progress, needs to be carried out by considering other aspects in detail, such as temporal and spatial resolution, radar calibration error using OSP-derived  $N0^*$  measurements, and error analysis related to the gauge network.

## REFERENCES

Iwanami K., E. Le Bouar, J. Tesud, M. Maki, R. Misum, S.G. Park and M. Suto, 2003: Application of the rain algorithm "ZPHI" to the X-band polarimetric radar data observed in Japan. Proceedings of the 31<sup>st</sup> Conf. on Radar Meteor. (6-12 Aug. 2003, Seattle, Washington, USA), Vol. 1, 274-276.

Le Bouar E., J. Testud and T.D. Keenan, 2001: Validation of the rain profiling algorithm "ZPHI" from the C-band polarimetric weather radar in

Darwin. J. Atmos. Oceanic Technol., 18, 1819-1837.

Testud J., E. Le Bouar, E. Obligis and M. Ali-Meheni, 2000: The rain profiling algorithm applied to polarimetric weather radar. J. Atmos. Oceanic Technol., 17, 332-356.